Haptic Exploration of Fine Surface Features

Allison M. Okamura and Mark R. Cutkosky
Dextrous Manipulation Laboratory
Stanford University
Stanford, CA 94305
{allisono, cutkosky}@cdr.stanford.edu

Abstract

In this paper we consider the detection of small surface features, such as ridges and bumps, on the surface of an object during dextrous manipulation. First we review the representation of object surface geometry and present definitions of surface features based on local curvature. These definitions depend on the geometries of both the robot fingertips and the object being explored. We also show that the trajectory traced by a round fingertip rolling or sliding over the object surface has some intrinsic properties that facilitate feature detection. Next, several algorithms based on the feature definitions are presented and compared. Finally, we present simulated and experimental results for feature detection using a hemispherical fingertip equipped with an optical tactile sensor.

1 Introduction

Haptic exploration is an important mechanism by which humans learn about the properties of unknown objects. Through the sense of touch, we are able to learn about characteristics such as object shape, surface texture, stiffness, and temperature. Unlike vision or audition, human tactile sensing involves direct interaction with objects being explored, often through a series of "exploratory procedures" [6]. Dextrous robotic hands are being developed to emulate exploratory procedures for the applications of remote planetary exploration, undersea salvage and repair, and other hazardous environment operations.

This paper focuses on a subset of haptic exploration: the sensing of small surface features such as cracks and bumps. Brown, et al. [2], define features as "application and viewer dependent interpretations of geometry." As we will show, the identification of a feature is not only dependent on the geometric properties of the object being explored, but also on the properties of the robotic finger performing the exploration.

Some of these features cannot be sensed accurately through static touch; motion is required. To excite the fast-acting, vibration sensitive mechanoreceptors embedded in the fingertips, humans roll and/or slide the fingertips over the surface [6]. Emulating this behavior presents a challenge in that manipulation must accomplish two tasks: (1) move the object to a desired location with a stable grasp and (2) move the fingers and sensors over the features.

In this work we consider first how features affect the path of a round fingertip rolling and/or sliding over an object surface. Although tactile sensors may be needed for manipulation control, we show that features can be detected using only the path of the fingertip center. We then present several algorithms for identifying surface features, with and without contact information from tactile sensors.

1.1 Previous Work

A number of investigators have addressed the problem of using robotic fingers in exploratory procedures. Examples include [1, 15, 16]. This work has mainly focused on the sensing of global object shapes and on fitting shapes to object models. The integration of tactile sensing and dextrous manipulation with rolling or sliding has also been addressed in recent work [9, 10, 15].

Much work on the identification of surface features has been done by researchers in the vision community. In early work, the definitions of features in applications such as topography were often ambiguous because they were based on natural language. More recently, researchers have developed definitions based on various mathematical models, including local maxima of pixels in a discrete 2D image, height or intensity graphs, and differential geometry (local extrema of principal curvatures or curvature properties of level sets of smooth functions) [4]. In another approach, Kunii, et al. [7] extended the idea of the Medial Axis Transform to develop skeletons of object shape and used caustic singularities to determine the locations of ridges. Applications of ridge detection include medical imaging [13] and the analysis of topographic data [8].

2 Defining Surface Features

This paper will take a differential geometry based approach to surface feature definition. In this section,

we will briefly review a mathematical description of an object surface and define the surfaces associated with the path of a round finger rolling or sliding over the object surface. Next, we define several features in the context of robotic haptic exploration. Finally, we provide an example of a three-dimensional surface feature.

2.1 Mathematical Background

Montana [14] defines a *Gauss map* for a manifold S as a continuous map $g : S \to S^2 \subset \mathcal{R}^3$ such that for every $s \in S$, $g(s)$ is perpendicular to S at s. The pair (f, U), where f is the invertible map $f : U \to S \subset \mathcal{R}^3$, is a coordinate system for S. The normalized *Gauss frame* at a point $\mathbf{u} = (u, v) \in U$ is defined as the coordinate frame with origin at $f(\mathbf{u})$ and coordinate axes

$$\begin{aligned} \mathbf{x}(\mathbf{u}) &= \frac{f_u(\mathbf{u})}{||f_u(\mathbf{u})||} \\ \mathbf{y}(\mathbf{u}) &= \frac{f_v(\mathbf{u})}{||f_v(\mathbf{u})||} \\ \mathbf{z}(\mathbf{u}) &= g(f(\mathbf{u})). \end{aligned} \tag{1}$$

The curvature form K is the 2×2 matrix

$$K = \begin{bmatrix} \mathbf{x}(\mathbf{u})^T \\ \mathbf{y}(\mathbf{u})^T \end{bmatrix} \begin{bmatrix} \frac{\mathbf{z_u}(\mathbf{u})}{||f_u(\mathbf{u})||} & \frac{\mathbf{z_v}(\mathbf{u})}{||f_v(\mathbf{u})||} \end{bmatrix}. \tag{2}$$

The principal curvatures $k_1(S)$ and $k_2(S)$ of the surface are the elements of the diagonalized curvature matrix K_d. The principal curvatures correspond to the $\mathbf{x}(\mathbf{u})$ and $\mathbf{y}(\mathbf{u})$ directions of the Gauss Frame.

Now consider a robotic finger with a spherical fingertip (surface S_f) with radius r_f following the contours of the surface. Using the formulation above, the curvature form for the fingertip is

$$K_f = \begin{bmatrix} \frac{1}{r_f} & 0 \\ 0 & \frac{1}{r_f} \end{bmatrix}. \tag{3}$$

As the finger traces over the surface of an object, the center point of the finger creates a *parallel surface*, S_p. This concept is also related to the offset surface as defined in CNC toolpath planning and other applications [17]. Figure 1 shows a 2D slice of a surface with several features and the parallel surface created by a spherical fingertip tracing over it.

The parallel surface is defined as the envelope of spheres whose centers are on the surface. A simple way to construct it is to draw a normal line (determined by the z-axis of the Gauss frame, $\mathbf{z}(\mathbf{u})$) with length r_f at each point on the surface. The locus of the end points is the parallel surface. $\mathbf{s}_p(\mathbf{u}) \in S_p$ maps U to $\mathcal{R}^3$:

$$\mathbf{s}_p(\mathbf{u}) = f(\mathbf{u}) + r_f \mathbf{z}(\mathbf{u}). \tag{4}$$

where $\mathbf{z}(\mathbf{u})$ is the z-direction of the Gauss frame, r_f is the radius of the fingertip, and $\mathbf{u}$ parameterizes the surface.

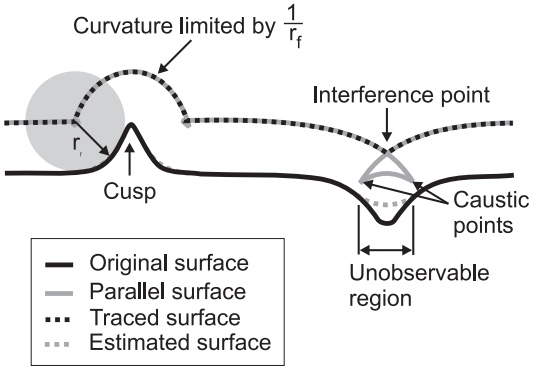

Figure 1: 2D slice of a spherical fingertip with original, parallel, traced, and estimated surfaces

In some cases, however, the actual surface created by moving a finger over the surface is not described by this equation. When the curvature of the surface is greater than that of the finger, the parallel surface has singularities known as *caustics* [8], even if the original surface is smooth. The presence of caustics indicates that the finger cannot exactly follow the contours of the object.

As shown in Figure 1, the caustic points bracket the area of the parallel surface where one of the original surface curvatures, $k_i(S)$, is greater than that of the finger, $\frac{1}{r_f}$. Due to interference, however, the path of an actual finger tracing over the surface is limited before the region bracketed by the caustics. The *interference point* is defined as the point where the finger can no longer follow the parallel surface when entering a region of $k_i(S) < -\frac{1}{r_f}$. Any curve on the parallel surface that travels in and out of a continuous area with $k_i(S) < -\frac{1}{r_f}$ must travel through two interference points. We define the *traced surface*, S_t, as the parallel surface without the portions that the fingertip cannot access due to curvature and interference limitations. A traced surface will always have a discontinuity at the interference point. Figure 1 shows interference points (discontinuities in the traced surface) and caustic points (discontinuities in the parallel surface), as well as the regions of the traced surface that round or fillet the object surface.

2.2 A New Feature Definition

Using the surface and parallel surface descriptions developed above, a new feature definition can be created for the purposes of feature identification and location. The concept of a feature in the context of haptic exploration with robotic fingers is not only dependent on the surface of the object, but also on the size and shape of the finger. In this paper, we assume a spherical fingertip.

We begin by defining a *curvature feature*, then use this as a building block to define *macro features*. Sup-

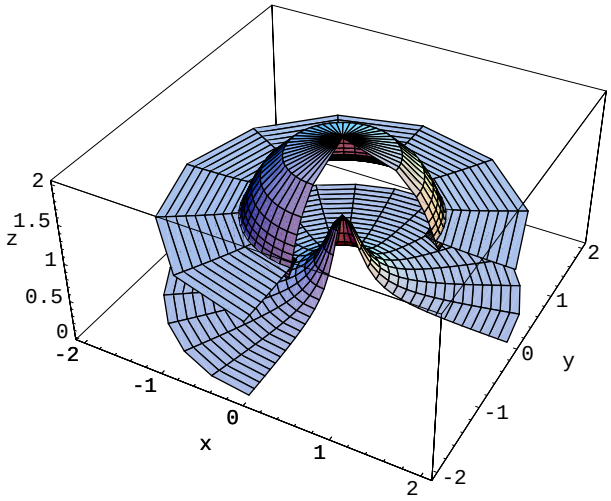

Figure 2: A bump feature (bottom), with parallel surface (top)

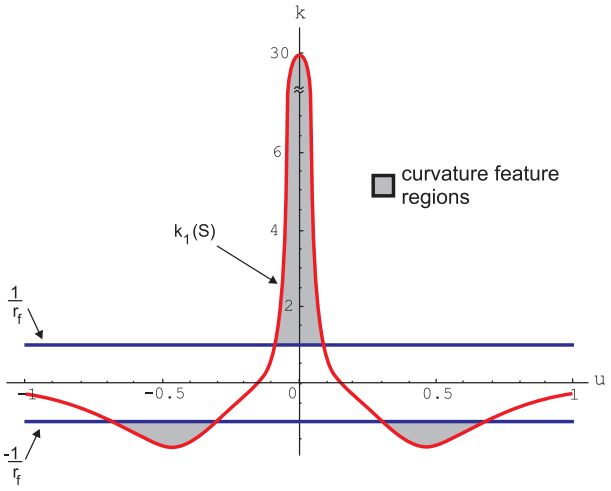

Figure 3: Curvature features are identified where $|k_i(S)| > \frac{1}{r_f}$

pose that an object can be locally fit with a surface S with principal curvatures $k_1(S)$ and $k_2(S)$. The basic criterion for defining a feature is maximum principal curvature:

Definition 1 *A* curvature feature, *as detected by a spherical robotic fingertip with radius r_f tracing over a surface S with curvature K, is a region where one of the principal curvatures satisfies $k_i > \frac{1}{r_f}$ or $k_i < -\frac{1}{r_f}$. These are* positive curvature *(convex) and* negative curvature *(concave) features, respectively.*

This means that the magnitude of the radius of curvature of the fingertip is larger than that of the feature. The simple definition above can be extended to define macro features, which consist of patterns of curvature features. For example:

Definition 2 *A* bump feature *is an area with one of the principal curvatures k_i following the pattern {negative curvature feature}{positive curvature feature}{negative curvature feature} as the finger travels over the surface.*

Definition 3 *A* ridge feature *is an area with principal curvature k_1 following the pattern {negative curvature feature}{positive curvature feature}{negative curvature feature} and $k_2 < \frac{1}{r_f}$. The ends of the ridge feature are defined when the second principal curvature k_2 follows the pattern {positive curvature feature}{negative curvature feature}.*

These definitions can be extended to additional compound features, however that is beyond the scope of this paper.

2.3 Example: A Bump Feature

Consider the three-dimensional parabolic surface of revolution "bump" shown in Figure 2. The bump surface is defined by the set

$$U = \{(u, v) | -1 < u < 1, 0 < v < \pi\} \tag{5}$$

and the map

$$\begin{aligned} &f : U \to \mathcal{R}^3, \\ &(u, v) \mapsto (u \cos v, u \sin v, \frac{1}{1 + au^2}) \end{aligned} \tag{6}$$

for some $a \in \mathcal{R}$.

It can be shown that (f, U) is an orthogonal coordinate system and thus the normalized Gauss frame exists for all $\mathbf{u} = (u, v) \in U$. For the bump example, the Gauss frame is

$$c = \sqrt{1 + \frac{4a^2u^2}{(1 + au^2)^4}} \tag{7}$$

$$d = 1 + au^2 \tag{8}$$

$$\begin{aligned} \mathbf{x}(\mathbf{u}) &= \left[\begin{array}{ccc} \frac{1}{c}\cos v & \frac{1}{c}\sin v & \frac{2au}{cd^2} \end{array} \right]^T \\ \mathbf{y}(\mathbf{u}) &= \left[\begin{array}{ccc} -\sin v & \cos v & 0 \end{array} \right]^T \\ \mathbf{z}(\mathbf{u}) &= \left[\begin{array}{ccc} \frac{2au}{cd^2}\cos v & \frac{2au}{cd^2}\sin v & \frac{1}{c} \end{array} \right]^T. \end{aligned} \tag{9}$$

The curvature matrix is

$$K = \left[\begin{array}{cc} \frac{2ad(1-3au^2)}{c(d^4+4a^2u^2)} & 0 \\ 0 & \frac{2a}{cd^2} \end{array} \right]. \tag{10}$$

Using the simplification variables c and d defined in Equations (7) and (8), the parallel surface is defined

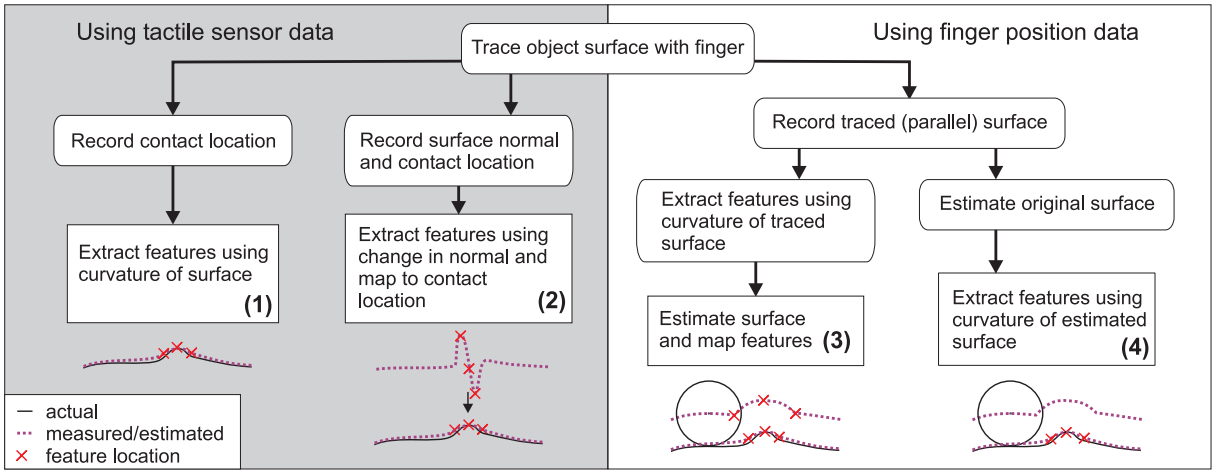

Figure 4: Algorithms for feature detection

by points

$$\mathbf{s}_p(\mathbf{u}) = \begin{bmatrix} (u + \frac{2ar_f u}{d^2 c}) \cos v \\ (u + \frac{2ar_f u \sin v}{d^2 c}) \sin v \\ \frac{1}{d} + \frac{r_f}{c} \end{bmatrix}. \qquad (11)$$

To determine the locations of the curvature features, we can plot the principal curvatures of the object surface and the robotic fingertip with respect to the variable u. Figure 3 shows the principal curvature $k_1(S)$ (the K_{11} element of the matrix in Equation 10) and $\pm\frac{1}{r_f}$, where $r_f = 1$, plotted against u for $a = 15$. There are three curvature features: two negative, and one positive. The pattern of curvature features can be identified as a bump as presented in Definition 2.

3 Feature Detection

In this section we present algorithms for detecting features using the surface feature definitions.

Figure 4 shows how position and tactile sensor data from the fingertip can be used to determine the features and global shape of the surface. Different chains on the diagram result in different identification algorithms. The algorithms can be divided into two groups: those that use tactile sensor data to determine the object surface and features, and those that use finger position data.

3.1 Using Tactile Sensor Data

Using the tactile sensor data and a model of the robot finger, one can compute the trajectory of the finger/object contact point in space and build a model of the surface, which we will call the *estimated surface*. This method works for any fingertip shape, as long as the contact point can accurately be sensed. [1]

[1] In fact, most tactile sensors are somewhat noisy and of low resolution and bandwidth compared to joint angle and force sensors, so the contact location data are not highly accurate.

The first algorithm (1) in Figure 4 calculates the curvature at each point on the estimated surface using any numerical difference method. Depending on the noise in the data, the points on the estimated surface may first need to be smoothed or fit to an analytical model before differentiation. Points on the smoothed or modeled surface with a curvature greater that that of the fingertip may then be identified as features.

The second algorithm (2) in Figure 4 requires that the normal of the surface be recorded over time. With a spherical fingertip, this is easily determined from the contact point on the finger. Again, due to noise in the sensor or position of the robot finger, the normal may need to be smoothed. The normal is then differentiated with respect to arclength, providing a spike at the location of the feature. This location can then be mapped to the estimated surface. This method uses the same information as the first algorithm, but improves feature detection because it uses a directly sensed quantity (the surface normal) rather than than the derivative of a noisy surface estimation.

3.2 Using Fingertip Center Position Data

Feature detection can also be accomplished without tactile sensor data, using the traced surface. If the fingertip is spherical (in 3D) or circular (in 2D), the traced surface created by the center of the fingertip can be used to estimate the original surface without tactile sensor data.

Estimation of the original surface can be done in several ways. Just as the theoretical parallel surface can be calculated from the original surface as in Equation (4), the estimated surface points $\mathbf{s}_e(\mathbf{u}) \in \mathcal{R}^3$ can be determined from the traced surface using

$$\mathbf{s}_e(\mathbf{u}) = \mathbf{s}_t(\mathbf{u}) - r_f \mathbf{z}_t(\mathbf{u}), \qquad (12)$$

where $\mathbf{s}_t(\mathbf{u})$ are points on the traced surface, $\mathbf{z}_t(\mathbf{u})$ is the z-direction or the Gauss frame of the traced sur-

face, r_f is the radius of the fingertip, and $\mathbf{u}$ parameterizes the surface. This method, however, is very susceptible to noise in $\mathbf{z}_t(\mathbf{u})$. Before calculating $\mathbf{z}_t(\mathbf{u})$, an improved estimation of the surface can be obtained by fitting a curve to or smoothing the traced surface.

The third algorithm (3) in Figure 4 extracts the features based only on the curvature of the traced surface. This has an advantage over the previous methods because the traced surface is likely to be less noisy than the estimated surface which used tactile sensor data. In addition, the traced surface will show interference points, which are a good indicators of features because they are discontinuities in the traced surface. This serves to enhance negative curvature features.

The fourth algorithm (4) in Figure 4 is similar to the previous algorithm, although the order of surface estimation and feature detection is switched. Now we use the traced surface to estimate the original surface first, and then perform feature detection using the curvature of the estimated surface.

3.3 Smoothing Data Using Curvature Limitations

For algorithms that use only the position of the fingertip, two nonlinear smoothing algorithms based on curvature limitations can be used to smooth noisy data in the traced and estimated surfaces. The algorithms apply the observations in Section 2.1 that the traced surface must round sharp cusps or corners on the object surface and fillet sharp indentations.

At each point on the traced and estimated surfaces, the principal curvatures are calculated using a numerical difference method. On the traced surface, any points for which $k_i(S_t) > \frac{1}{r_f}$ are invalid (i.e., they cannot correspond to motion along an object surface) and should be deleted. After removing these points, the traced surface can be smoothed by a standard smoothing method. After the traced surface is smoothed, the estimated object surface is calculated using the *envelope* of r_f circles centered on the traced surface. In the estimated surface, the principal curvature $k_i(S_t)$ must be at least $-\frac{1}{r_f}$. Although the actual object surface could have regions with larger negative curvature, it is impossible for the fingertip to detect such regions. Again, such points should be deleted and the remaining surface can be smoothed using any standard method.

4 Simulation and Experiments

4.1 Simulated Data

A realistic simulation of a spherical fingertip traveling over a step shows the curvature limitations in surface estimation. For the purposes of simulation, a realistic traced surface must be calculated. First, the parallel surface is calculated from the original surface, then the interference points are identified and the unreachable points are removed to form the traced surface. Next, because points on the parallel surface are not spaced equally, the surface is re-calculated using equal arclengths between the points. Finally, Gaussian noise with a variance of 0.01 is added for realism.

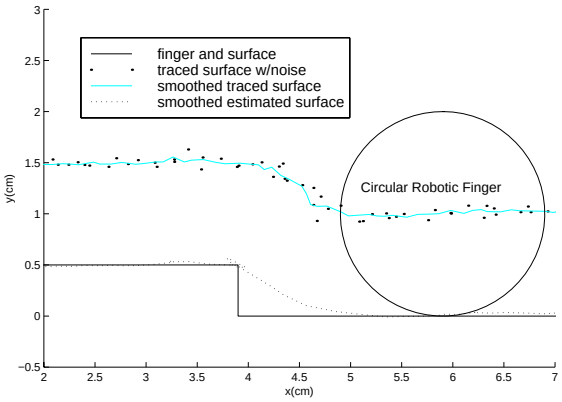

Figure 5: Simulated data of a finger tracing over a step

Now we invoke the nonlinear smoothing algorithms to limit the curvature to realistic values. The first curvature limitation algorithm is used to remove unreachable points from the traced surface, then it is smoothed. Then, the original surface is estimated using the envelope of circles with centers on the smoothed traced surface. Next, the second curvature limitation algorithm is used to remove unreachable points from the estimated surface. As a final step, the surface can be fit to create an analytical model. Figure 5 shows a 2D slice of four surfaces in this example: the object surface, the traced surface with noise, the smoothed traced surface, and the smoothed estimated object surface.

4.2 Experiments

4.2.1 Apparatus

Manipulation experiments were performed using two degree-of-freedom robotic fingers and tactile sensors developed by Maekawa, et al. [11, 12]. The optical waveguide tactile sensors on the fingers form a hemispherical fingertip and provide analog signals that can be used to calculate the intensity and centroid of the contact point(s). The 20 mm diameter sensors can be sampled at 5 kHz, and have a field of detection of ± 75 degrees from the sensor pole. The error is aproximately ± 1 degree, although this can change when the contact area increases during sliding. A calibration was performed to characterize and remove the nonlinearity of the sensor.

As is typical of many robotic fingers, the workspace was limited and thus a combination of rolling and slid-

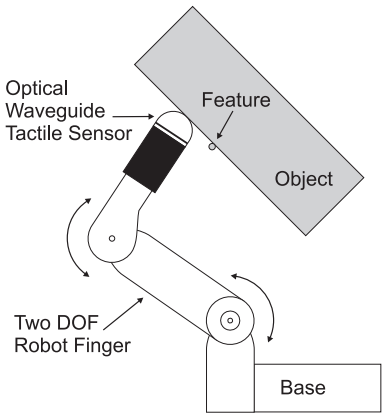

Figure 6: Experimental Apparatus

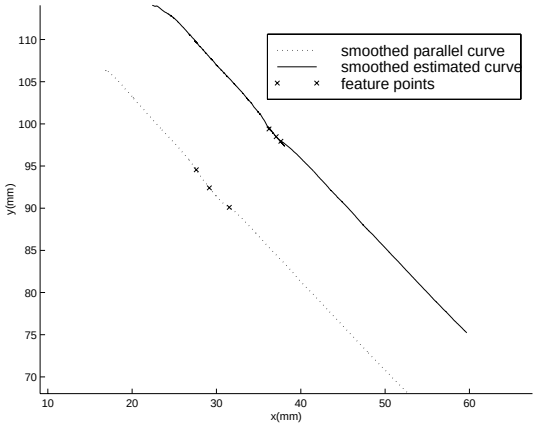

Figure 7: Feature detection with a robotic finger rolling/sliding on a 45° surface with a 0.65 mm bump feature

ing was necessary to move the fingers over the surface of the object. A hybrid force/velocity control was used to obtain smooth sliding over flat surfaces with bump features (0.5-1.5 mm wires placed on the surface).

During motion, joint angle potentiometers were used to determine the position of the center of the hemispherical fingertip. The location of the contact point on the fingertip was then used to determine the direction of the contact normal, which was filtered to reduce noise. The center of the fingertip can be sensed to within ± 0.2 mm and the contact location can be estimated within ± 0.5 mm. A tension differential-type torque sensor is used to measure torque in the joints and calculate the cartesian force at the fingertip.

Because the fingertip is spherical, the contact location on the finger gives the tangent and normal of the rigid surface. The velocity of the fingertip tangent to the surface and the force normal to the surface were controlled using a simple proportional law. The finger moved with an average speed of 0.03 m/sec and a normal force of 1 ± 0.01 N.

4.2.2 Results

Each of the algorithms outlined in Figure 4 was tested using the data from these experiments. Algorithm (1) often resulted in false negative identifications because the estimated surface was obtained directly from the contact point. Concave curvature features on the object were overlooked because of curvature limitations; the data are these points are automatically smoothed to the radius of curvature of the fingertip. Using algorithm (2), spikes in the contact normal indicated the presence of negative curvature (concave) features. This method does not provide good detection of positive (convex) features, because the normal direction does not change as quickly at those points.

Using algorithm (3), features were extracted using the curvature of the traced surface, then mapped to an estimated surface. This algorithm performed the best for our application of small bump features on a flat surface. Figure 7 shows the traced and estimated surfaces and features detected for a bump on a flat surface angled at 45 degrees, with a 0.65 mm diameter wire stretched across the surface. Figure 8 shows a close up view of the unsmoothed estimated object surface data in a region with no features. The orientation of the object is the same as that in Figure 6. Algorithm (4) resulted in false negatives for the same reason as algorithm (1): using the estimated surface to determine locations with high curvature is not feasible because of the curvature limitations.

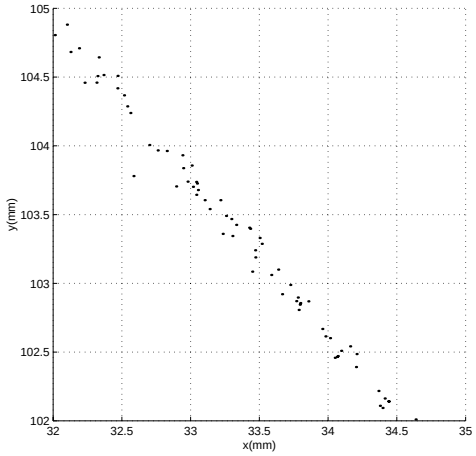

Figure 8: Close up of estimated object surface data

5 Conclusions and Future Work

In this work, we have defined features for the context of robotic haptic exploration with curved fingertips. Features may be identified using the curvatures

of traced or estimated surfaces, without tactile sensor data. In particular, the traced surface described by a rounded fingertip accentuates concave features on the object surface. This is an interesting result because, while we may need contact location data for stable manipulation control, we do not need them to recreate the object shape or to identify small surface features with round fingertips. We also presented definitions for curvature and macro surface features in this context and methods for smoothing data based on the inherent curvature limitations of the physical system.

One area for future work is the development of 3D haptic exploratory procedures that take advantage of the feature definitions. For example, if a fingertip encounters a ridge, some specific strategies may be used to determine the size and extent (length) of the feature. Another possible direction for this work is fitting the features onto a global object model. If the general shape of the object is fit to some simple surface, it should be possible to add the details of fine surface features using a simple data structure. Finally, we are studying the display the object global shape and fine surface features using force- and vibration-feedback.

Acknowledgments

This work was supported by NSF dissertation enhancement award 9724763 and STRICOM grant M67004-97-C-0026 through Immersion Corporation. Special thanks are given to Dr. Kazuo Tanie for hosting Ms. Okamura's stay at the Mechanical Engineering Lab in Tsukuba, Japan, and Dr. Hitoshi Maekawa for providing the experimental apparatus.

References

[1] P.K. Allen and P. Michelman, "Acquisition and Interpretation of 3-D Sensor Data from Touch," *IEEE Trans. on Robotics and Automation*,Vol. 6 No. 4, pp. 397-404, 1990.

[2] K.N. Brown, C.A. McMahon, and J.H. Sims Williams, "Features, aka The Semantics of a Formal Language of Manufacturing," *Research in Engineering Design*, Vol. 7, No. 3, pp. 151-172, 1995.

[3] R.D. Howe and M.R. Cutkosky, "Touch Sensing for Robotic Manipulation and Recognition," *The Robotics Review 2, O. Khatib*, J. Craig and T. Lozano-Perez, eds., M.I.T. Press, Cambridge, MA, pp. 55-112, 1992.

[4] D. Eberly, et al., "Ridges for Image Analysis," *Journal of Mathematical Imaging and Vision*, Vol. 4, pp. 353-373, 1994.

[5] R.E. Ellis, "Extraction of Tactile Features by Passive and Active Sensing," *Intelligent Robots and Systems*, D.P. Casasent, Ed., 1984.

[6] R.L. Klatzky and S. Lederman, "Intelligent Exploration by the Human Hand," Chapter 4, *Dextrous Robot Manipulation*, S.T. Venkataraman and T. Iberall, eds., Springer-Verlag, 1990.

[7] T.L. Kunii, et al., "Hierarchic Shape Description via Singularity and Multiscaling," *Proc. of the 18th Annual Intl. Comp. Software and Applications Conf. (COMPSAC 94)*, Taipei, Taiwan, pp. 242-251, 1994.

[8] I.S. Kweon and T. Kanade, "Extracting Topographic Terrain Features from Elevation Maps," *CVGIP: Image Understanding*, Vol. 59, No. 2, pp. 171-182, 1994.

[9] Z.X. Li, Z. Qin, S. Jiang and L. Han, "Coordinated Motion Generation and Real-time Grasping Force Control for Multifingered Manipulation," *Proc. IEEE Intl. Conf. on Robotics and Automation*, pp. 3631-3638, 1998.

[10] H. Maekawa, K. Tanie, and K. Komoriya, "Tactile Sensor Based Manipulation of an Unknown Object by a Multifingered Hand with Rolling Contact," *Proc. 1995 IEEE Intl. Conf. on Robotics and Automation*, pp. 743-750, 1995.

[11] H. Maekawa, et al., "Development of a Three-Fingered Robot Hand with Stiffness Control Capability," *Mechatronics*, Vol. 2, No. 5, pp. 483-494, 1992.

[12] H. Maekawa, K. Tanie, and K. Komoriya, "A Finger-Shaped Tactile Sensor Using an Optical Waveguide," *Proc. 1993 IEEE Intl. Conf. on Systems, Man and Cybernetics*, pp. 403-408, 1993.

[13] J.B.A. Maintz, P.A. van den Elsen and M.A. Viergever, "Evaluation of Ridge Seeking Operators for Multimodality Medical Image Matching," *IEEE Trans. of Pattern Analysis and Machine Intelligence*, Vol. 18, No. 4, pp. 353-365, 1996.

[14] D.J. Montana, "The Kinematics of Contact and Grasp," *Intl. Journal of Robotics Research*, Vol. 7, No. 3, pp. 17-32.

[15] A.M. Okamura, M.L. Turner and M.R. Cutkosky, "Haptic Exploration of Objects with Rolling and Sliding," *Proc. 1997 IEEE Intl. Conf. on Robotics and Automation*, Vol. 3, pp. 2485-2490, 1997.

[16] K. Pribadi, J.S. Bay, and H. Hemami, "Exploration and Dynamic Shape Estimation by a Robotic Probe," *IEEE Trans. on Systems, Man, and Cybernetics*, Vol. 19, No. 4, pp. 840-846, 1989.

[17] J.R. Rossignac and A.A.G. Requicha, "Offsetting Operations in Solid Modeling," *Computer Aided Geometric Design*, Vol. 3, No. 2, pp. 129-148, 1986.